Supporting Information

Two-dimensional Confined Polyoxometalate-based Chiral Luminescent Sensor for High Enantioselective Sensing

Guicong Hu,[a]‡ Zhaohui Wu,[a]‡ Ailin Cai,[a] Xinzhu Xing,[a] Wen Chang,[a] Qinglong Qiao,[b] Bo Qi*[a] and Yu-Fei Song*[ac]*

[a] State Key Laboratory of Chemical Resource Engineering, Beijing University of Chemical Technology, Beijing 100029 P. R. China. Email: bqi@mail.buct.edu.cn; songyf@mail.buct.edu.cn;

[b] Dalian Institute of Chemical Physics, Chinese Academy of Sciences 457 Zhongshan Road, Dalian 116023, China. Email: qqlqiao@dicp.ac.cn;

[c] Quzhou Institute for Innovation in Resource Chemical Engineering, Quzhou, Zhejiang Province, 324000 P. R. China.

‡: These authors contributed equally to this work.

CONTENTS

Section 1 Experimental Section

Section 2 Characterizations of Chiral Fluorescence Sensor

Section 1 Experimental Section

1.1 Preparation of Mg_3Al-EuW_{10}. Mg_3Al-EuW_{10} was synthesized via the step-by-step assembly process. Mg_3Al-NO_3 (0.3 g) was dispersed in formamide (300 mL), and the mixture was stirred under nitrogen for 48 h to form a suspension with the Tyndall effect. $Na_9EuW_{10}O_{36}\cdot 32H_2O$ (0.33 mmol) was dissolved in deionized water (5 mL) and added dropwise to the reaction mixture. After stirred for five minutes to form a white precipitate, the solid products were collected by filtration and washed with deionized water and ethanol, then dried in a vacuum oven at 60 °C for 48 h.

1.2. Preparation of *L*-CIL-Mg_3Al-NO_3. *L*-CIL-Mg_3Al-NO_3 was synthesized via the step-by-step assembly process. Mg_3Al-NO_3 (0.3 g) was dispersed in formamide (300 mL), and the mixture was stirred under nitrogen for 48 h to form a suspension with the Tyndall effect. *L*-CIL (2.64 mmol) was dissolved in CH_2Cl_2 (2 mL) and added dropwise to the above clear and transparent hydrotalcite nanosheet solution. The reaction mixture was stirred under N_2 for 24 h. $NaNO_3$ (38 mmol) was dissolved in deionized water (10 mL) and added dropwise to the reaction mixture. After stirred for 12 h to form a white precipitate, the solid products were collected by filtration and washed with deionized water and ethanol, then dried in a vacuum oven at 60 ℃ for 48 h. Subsequently, the tert butoxycarbonyl deprotection was performed by thermal treatment of *L*-CIL-Boc-Mg_3Al-NO_3 at 150 °C under vacuum for 6 h.

1.3. Preparation of Control Fluorescence Quenching Material *L*-CIL-Mg_3Al-NO_3+EuW_{10}. *L*-CIL-Mg_3Al-NO_3+EuW_{10} was prepared via the electrostatic modification process. The *L*-CIL-Mg_3Al-NO_3 (100 mg, containing 3 μmol *L*-CIL) was dispersed in deionized water (100 mL) and stirred under N_2 for 5 min. Then, EuW_{10} solution (10 mL, 0.02 mM) was added to the suspension mentioned above. The mixture was stirred vigorously for 24 h and used as the control fluorescence quenching material for the later fluorescent chiral recognition of Cinchonine/Cinchonidine.

Section 2 Characterizations of Chiral Fluorescence Sensor

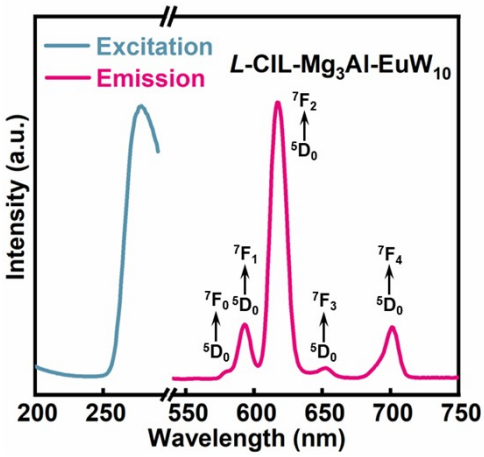

Fig. S1 Excitation and emission spectra of *L*-CIL-Mg_3Al-EuW_{10} in DMF.

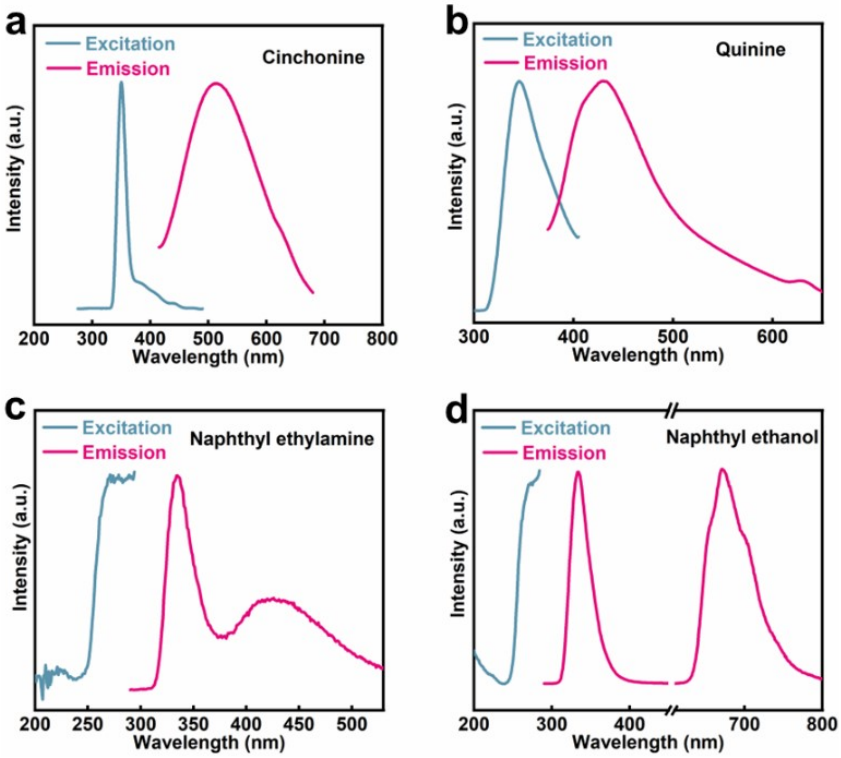

Fig. S2. Excitation and emission spectra of (a) Cinchonine, (b) Quinine, (c) Naphthyl ethylamine, and (d) Naphthyl ethanol in DMF.

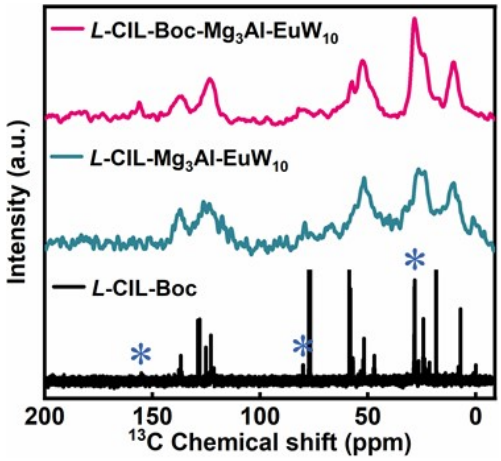

Fig. S3. ^{13}C NMR spectra of *L*-CIL-Boc-Mg_3Al-EuW_{10}, *L*-CIL-Mg_3Al-EuW_{10}, and *L*-CIL-Boc (*:Boc's peaks).

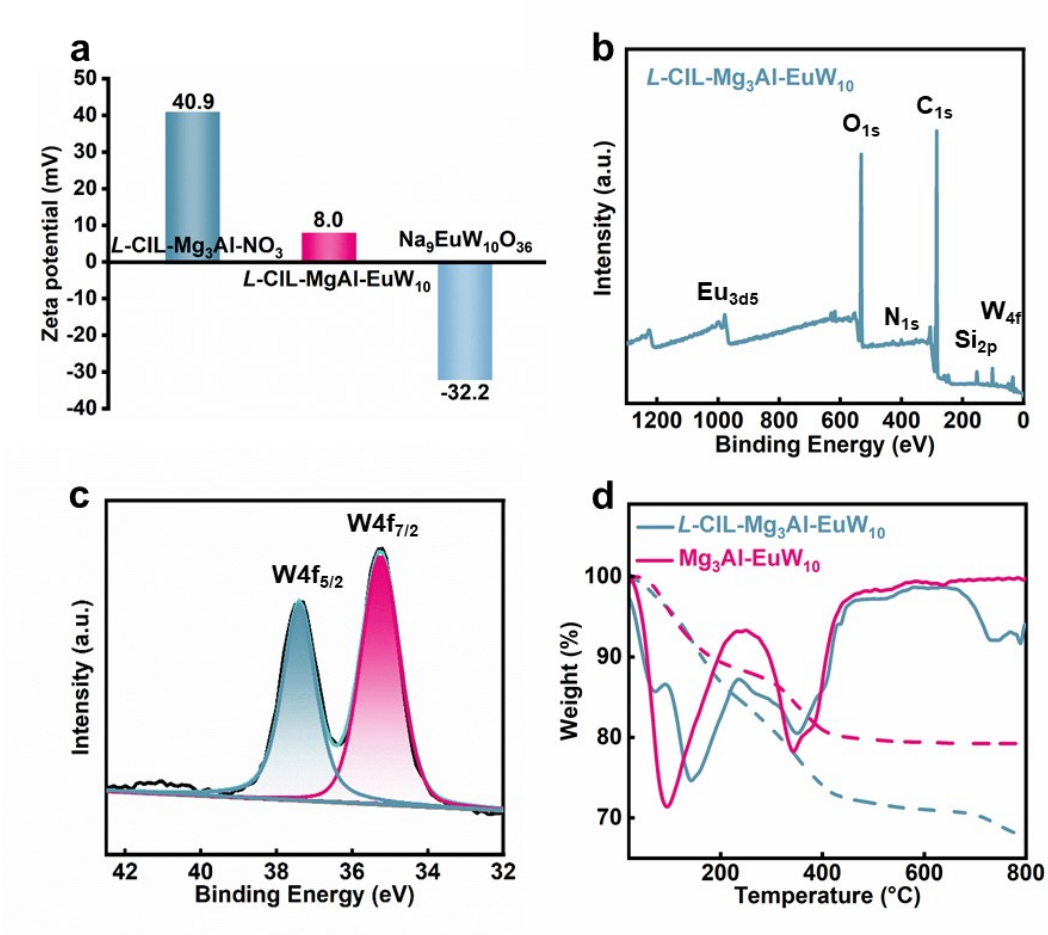

Fig. S4. (a) Zeta potentials of *L*-CIL-Mg_3Al-NO_3, *L*-CIL-Mg_3Al-EuW_{10}, and $Na_9EuW_{10}O_{36}$. (b) XPS survey spectrum of *L*-CIL-Mg_3Al-EuW_{10}. (c) XPS spectrum for the W 4f core level of *L*-CIL-Mg_3Al-EuW_{10}. (d) TG-DTG profile of Mg_3Al-EuW_{10} and *L*-CIL-Mg_3Al-EuW_{10}.

Table S1. The formulas of different materials

Entry	Sample	Formula
1	*L*-CIL-Mg_3Al-EuW_{10}	$Mg_{0.72}Al_{0.25}(OH)_{1.94}(EuW_{10}O_{36})_{0.034}$ $(O_3SiC_{11}H_9N_3)_{0.063}(NO_3)_{0.007}\cdot 0.63H_2O$
2	Mg_3Al-EuW_{10}	$Mg_{0.70}Al_{0.25}(OH)_{1.90}(EuW_{10}O_{36})_{0.026}[NO_3]_{0.016}\bullet 0.71H_2O$

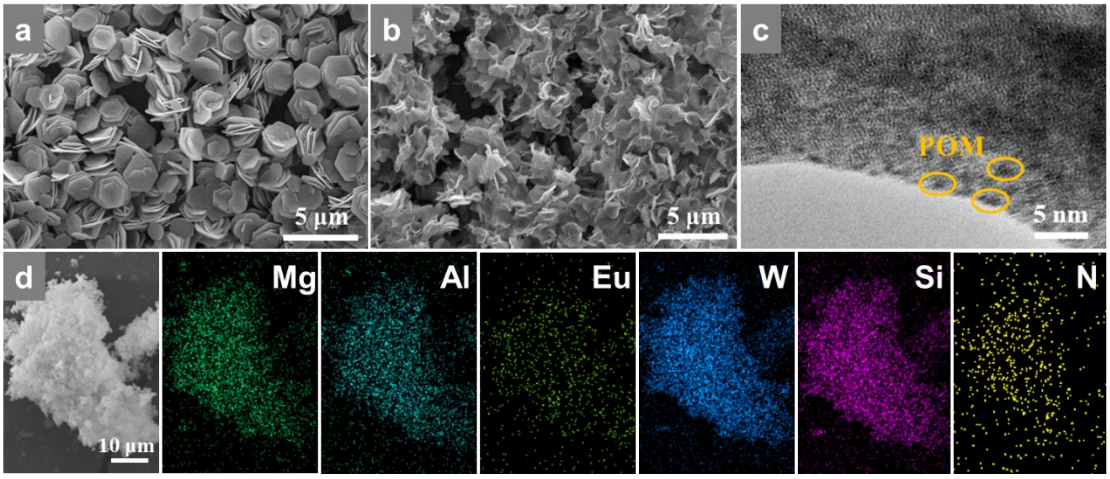

Fig. S5. SEM images of (a) Mg_3Al-NO_3 and (b) *L*-CIL-Mg_3Al-EuW_{10}. (c) HRTEM image of *L*-CIL-Mg_3Al-EuW_{10}. The yellow circles represented the highly dispersed EuW_{10} molecules. (d) SEM-EDX elemental mapping images of *L*-CIL-Mg_3Al-EuW_{10} for Mg, Al, Eu, W, Si, and N elements.

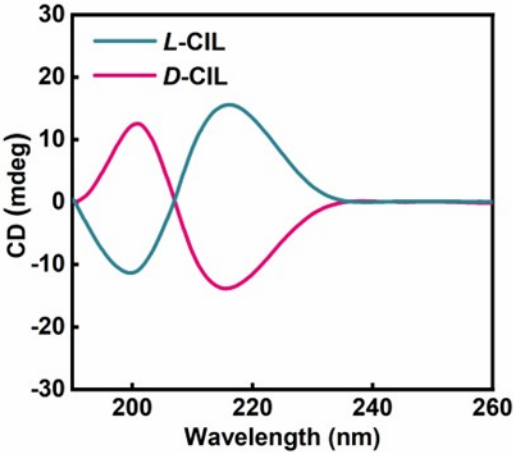

Fig. S6. CD spectra of *L*/*D*-CIL.

Table S2. Comparison of Physicochemical Properties of Mg_3Al-EuW_{10} and *L*-CIL-Mg_3Al-EuW_{10}.

Entry	Sample	S_{BET} (m^2/g)[a]	V_p (cm^3/g)[b]	D (nm)[c]
1	*L*-CIL-Mg_3Al-EuW_{10}	123.79	0.56	19.55
2	Mg_3Al-EuW_{10}	59.41	0.20	15.36

[a]S_{BET}, specific surface area calculated by the BET method in the relative adsorption pressure (P/P_0); [b]V_p, total pore volume determined by N_2 adsorption at relative pressure; [c]D, Pore diameter obtained from the desorption isotherm by the BJH method

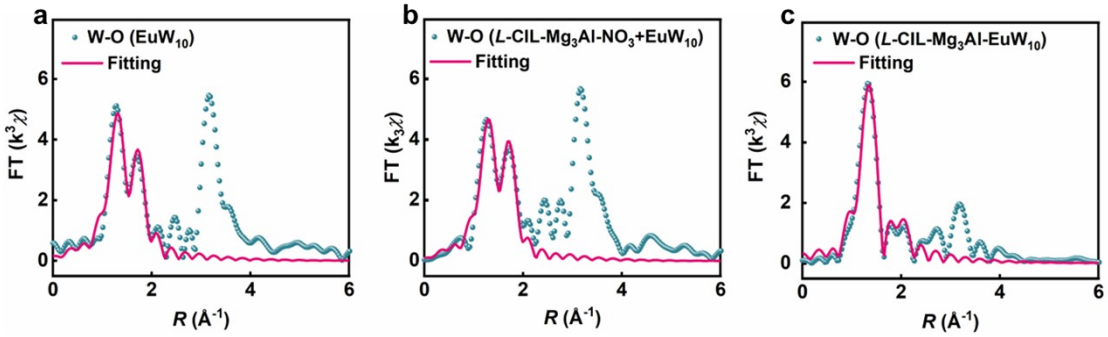

Fig. S7. Fourier transforms of the W L-edge EXAFS spectra for (a) EuW_{10}, *L*-CIL-Mg_3Al-NO_3 + EuW_{10} and *L*-CIL-Mg_3Al-EuW_{10}.

Table S3. Local structure parameters around W estimated by EXAFS analysis

Sample	Shell	N^a	S_0	$\sigma^2[10^{-3}Å^2]^b$	R[Å][c]	R-factor (10^{-3})
EuW_{10}	W-O_1	2.44	0.9	5.07	1.78	19.44
	W-O_2	2.62			1.96	
	W-O_3	0.90			2.28	
L-CIL-Mg_3Al-NO_3 + EuW_{10}	W-O_1	2.34	0.9	5.00	1.77	15.08
	W-O_2	2.69			1.96	
	W-O_3	0.96			2.28	
L-CIL-Mg_3Al-EuW_{10}	W-O_1	2.69	0.9	4.29	1.77	18.58
	W-O_2	1.84			1.98	
	W-O_3	1.44			2.21	

[a]N = coordination number; [b]R = average distance between absorber and backscatter atoms; [c]σ^2 = Debye-Waller factor

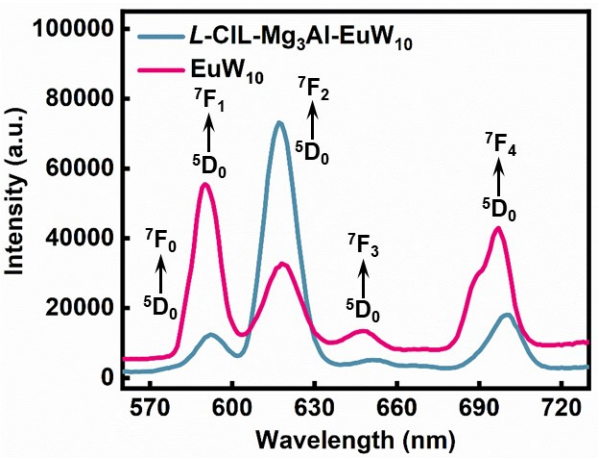

Fig. S8. Fluorescence spectra of *L*-CIL-Mg_3Al-EuW_{10} and EuW_{10}.

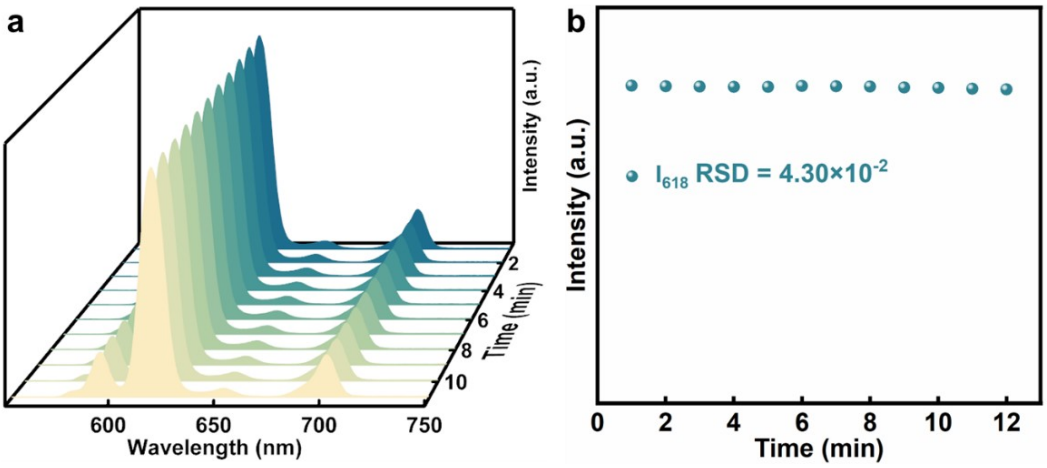

Fig. S9. Emission spectra (a) and luminescence intensities (b) of *L*-CIL-Mg_3Al-EuW_{10} suspensions in DMF for 12 minutes. RSD is relative standard deviation.

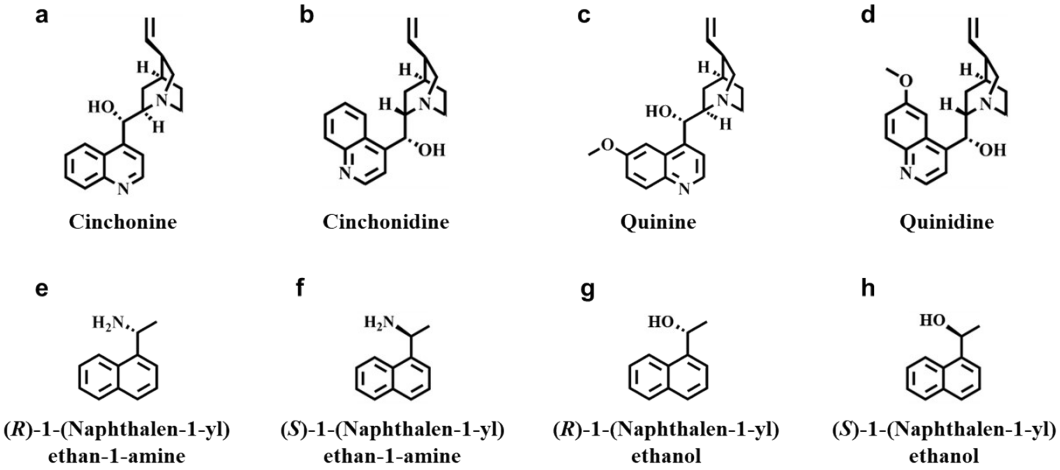

Fig. S10. The structures of the analytes. (a) Cinchonine and (b) Cinchonidine, (c) Quinine and (d) Quinidine, (e) *R*-Naphthyl ethylamine and (f) *S*-Naphthyl ethylamine, (g) *R*-Naphthyl ethanol and (h) *S*-

Naphthyl ethanol.

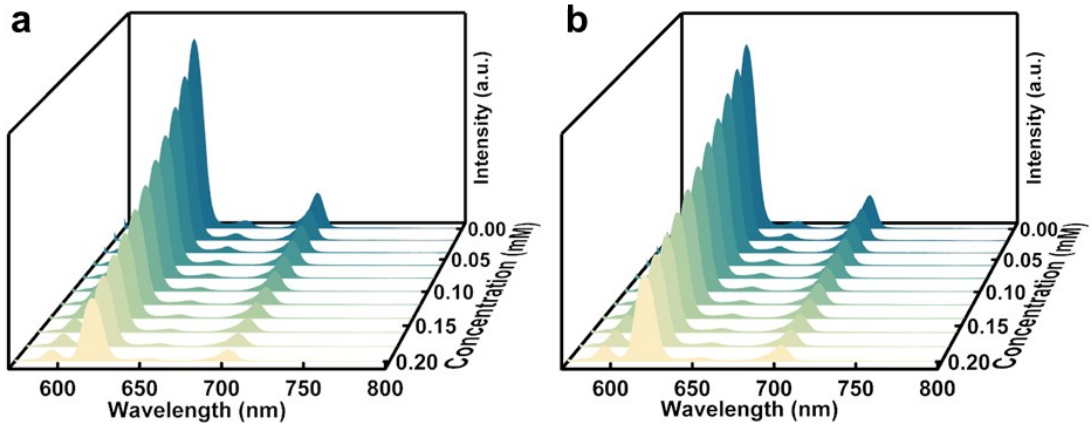

Fig. S11. Fluorescence emission spectra excited at 278 nm. *D*-CIL-Mg_3Al-EuW_{10} dispersed in DMF upon incremental addition of (c) Cinchonine and (d) Cinchonidine.

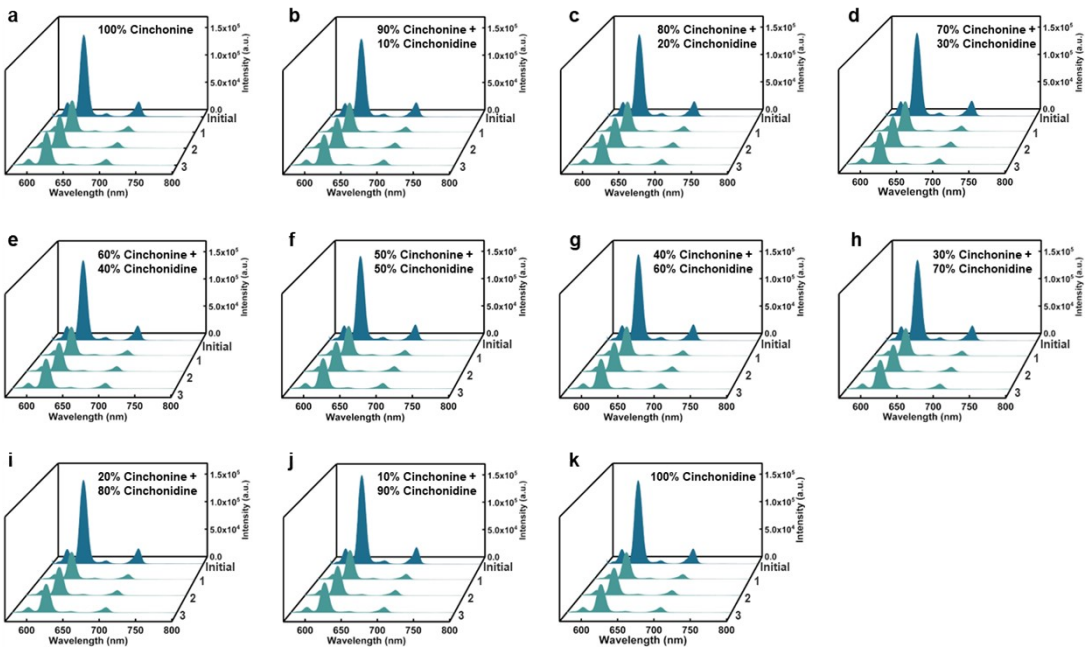

Fig. S12. Fluorescence intensity changes of *L*-CIL-Mg_3Al-EuW_{10} toward addition of a mixture of different proportions of Cinchonine and Cinchonidine. The initial lines represent the original *L*-CIL-Mg_3Al-EuW_{10} while others stand for *L*-CIL-Mg_3Al-EuW_{10} with the mixtures of different ee values for three times.

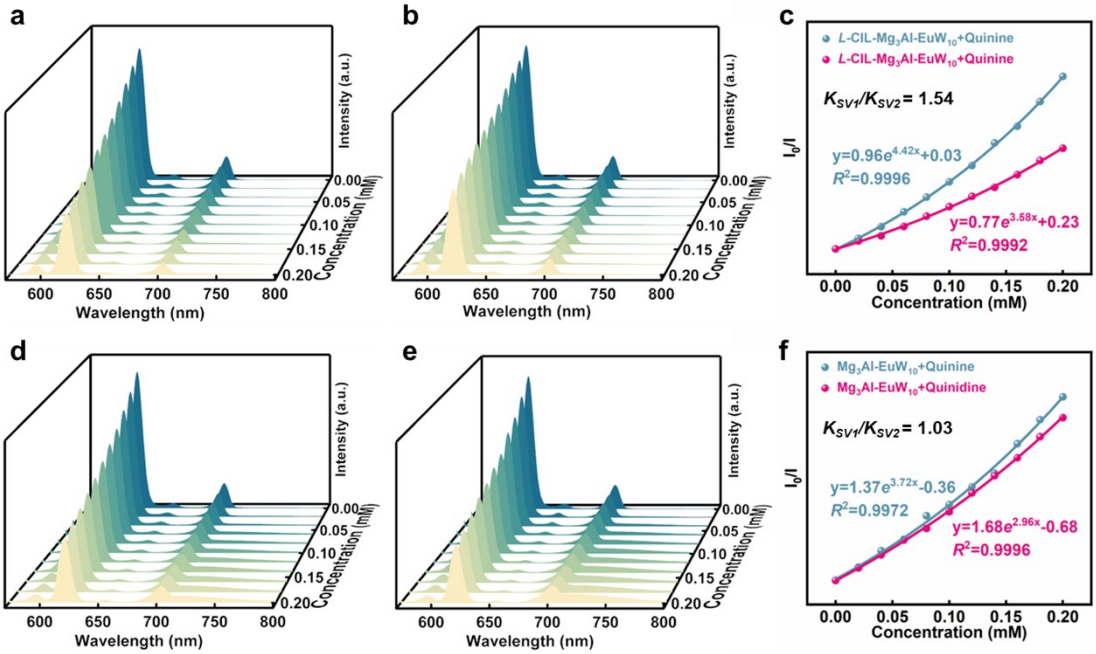

Fig. S13. Fluorescence emission spectra excited at 278 nm. *L*-CIL-Mg_3Al-EuW_{10} dispersed in DMF upon incremental addition of (a) Quinine and (b) Quinidine. (c) Fluorescence intensity changes of *L*-CIL-Mg_3Al-EuW_{10} at 618 nm. Mg_3Al-EuW_{10} dispersed in DMF upon incremental addition of (d) Quinine and (e) Quinidine. (f) Fluorescence intensity changes of Mg_3Al-EuW_{10} at 618 nm.

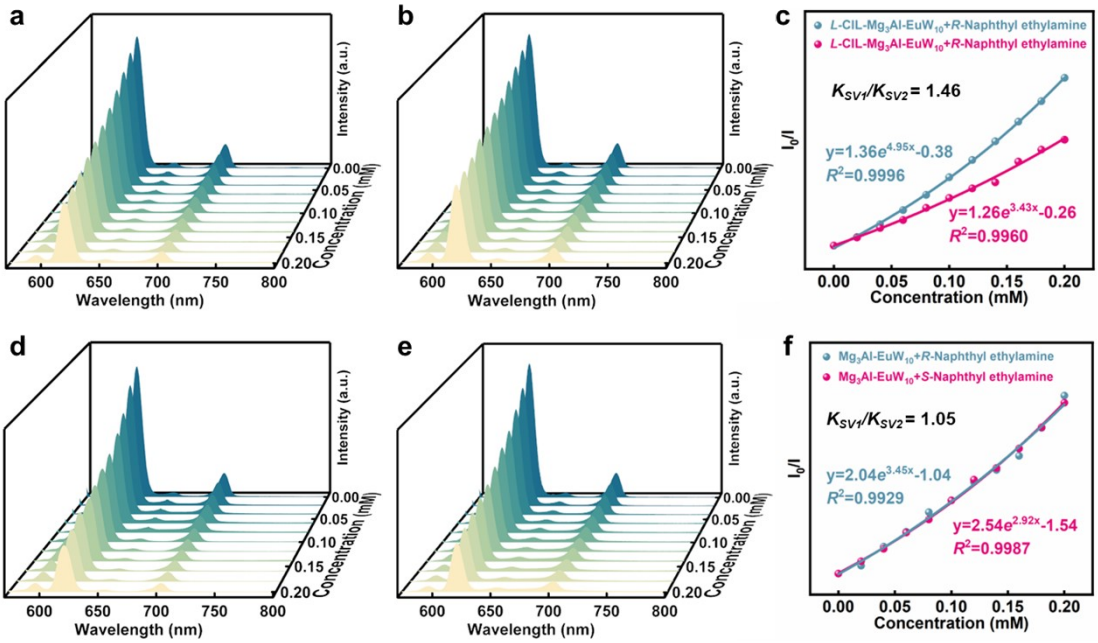

Fig. 14. Fluorescence emission spectra excited at 278 nm. *L*-CIL-Mg_3Al-EuW_{10} dispersed in DMF upon incremental addition of (a) *R*-Naphthyl ethylamine and (b) *S*-Naphthyl ethylamine. (c) Fluorescence intensity changes of *L*-CIL-Mg_3Al-EuW_{10} at 618 nm. Mg_3Al-EuW_{10} dispersed in DMF upon incremental addition of (d) *R*-Naphthyl ethylamine and (e) *S*-Naphthyl ethylamine. (f) Fluorescence intensity changes of Mg_3Al-EuW_{10} at 618 nm.

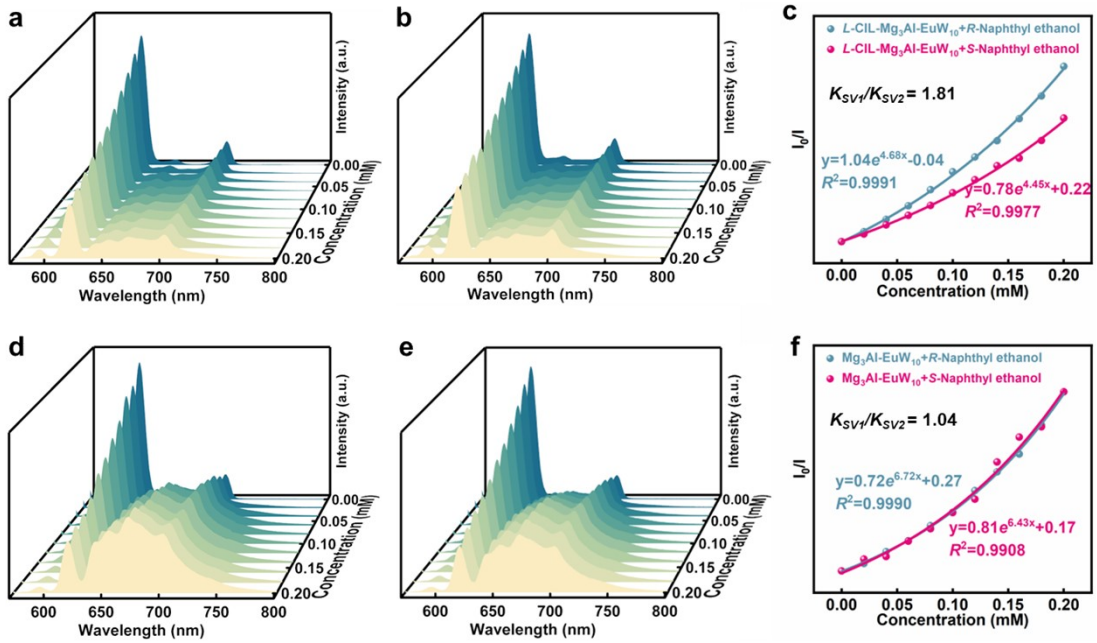

Fig. S15. Fluorescence emission spectra excited at 278 nm. *L*-CIL-Mg_3Al-EuW_{10} dispersed in DMF upon incremental addition of (a) *R*-Naphthyl ethanol and (b) *S*-Naphthyl ethanol. (c) Fluorescence intensity changes of *L*-CIL-Mg_3Al-EuW_{10} at 618 nm. Mg_3Al-EuW_{10} dispersed in DMF upon incremental addition of (d) *R*-Naphthyl ethanol and (e) *S*-Naphthyl ethanol. (f) Fluorescence intensity changes of Mg_3Al-EuW_{10} at 618 nm.

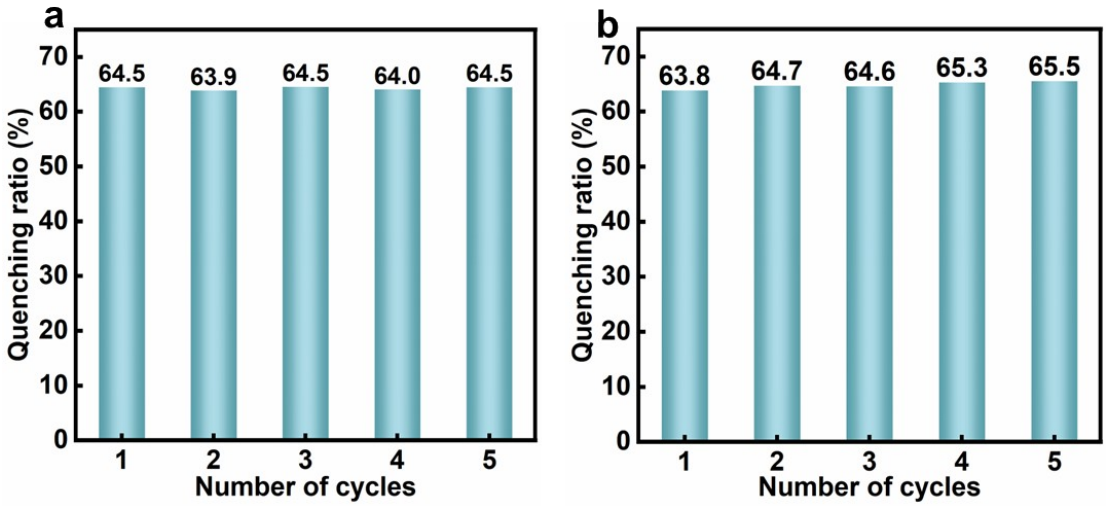

Fig. S16. Recycling experiment. Quenching ability of *L*-CIL-Mg_3Al-EuW_{10} dispersed in DMF in the presence of (a) Cinchonine and (b) Cinchonidine with five cycles (the intensity with 0.02 $mmol \cdot L^{-1}$ analytes, respectively) at 618 nm.

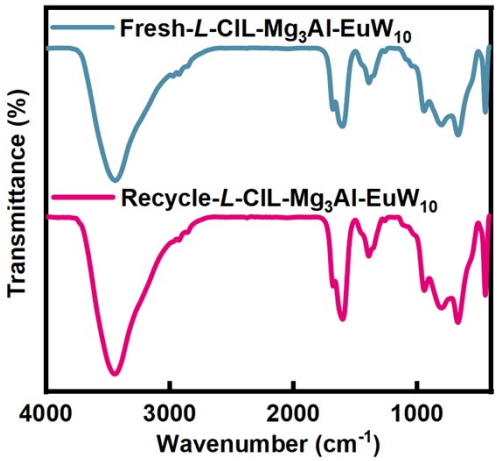

Fig. S17. FT-IR spectra of *L*-CIL-Mg_3Al-EuW_{10} fresh and recycle.

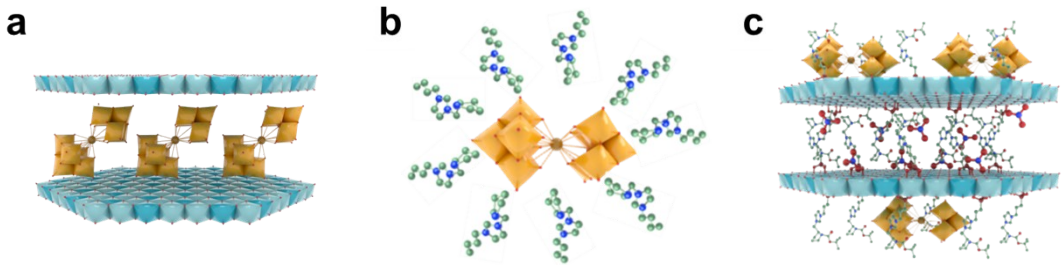

Fig. S18. (a) Model of Mg_3Al-EuW_{10}, the anionic EuW_{10} clusters were encapsulated within the interlayer of LDH. (b) Model of *L*-CIL + EuW_{10}, the anionic EuW_{10} clusters were encapsulated by the cationic chiral pyrrolidine-type ligands. (c) Model of *L*-CIL-Mg_3Al-NO_3 + EuW_{10}, the EuW_{10} clusters were distributed on the outer chiral surface of *L*-CIL-Mg_3Al-NO_3.

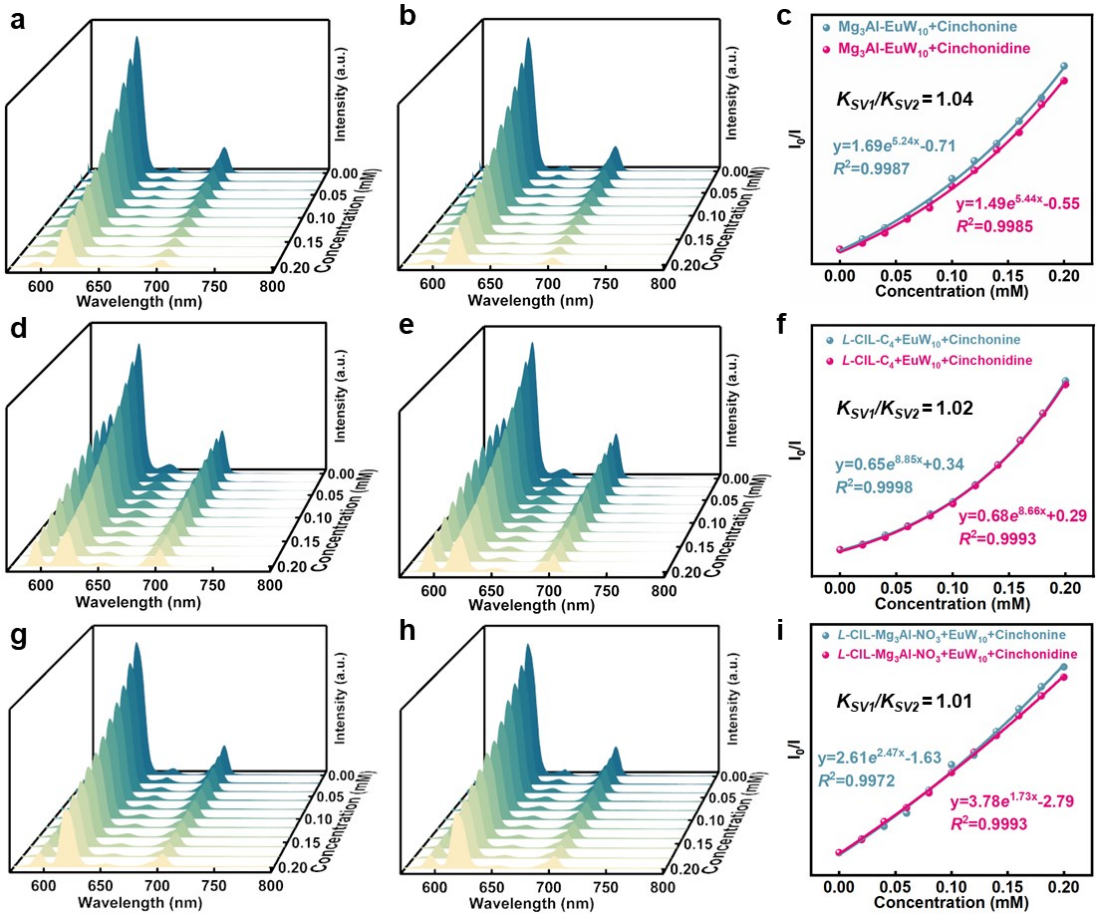

Fig. S19. Fluorescence emission spectra excited at 278 nm. Mg_3Al-EuW_{10} dispersed in DMF upon incremental addition of (a) Cinchonine and (b) Cinchonidine. (c) Fluorescence intensity changes of Mg_3Al-EuW_{10} at 618 nm. *L*-CIL-C_4 + EuW_{10} dissolved in DMF upon incremental addition of (d) Cinchonine and (e) Cinchonidine. (f) Fluorescence intensity changes of *L*-CIL-C_4 + EuW_{10} at 618 nm. *L*-CIL-Mg_3Al-NO_3 + EuW_{10} dispersed in DMF upon incremental addition of (g) Cinchonine and (h) Cinchonidine. (i) Fluorescence intensity changes of *L*-CIL-Mg_3Al-NO_3 + EuW_{10} at 618 nm.

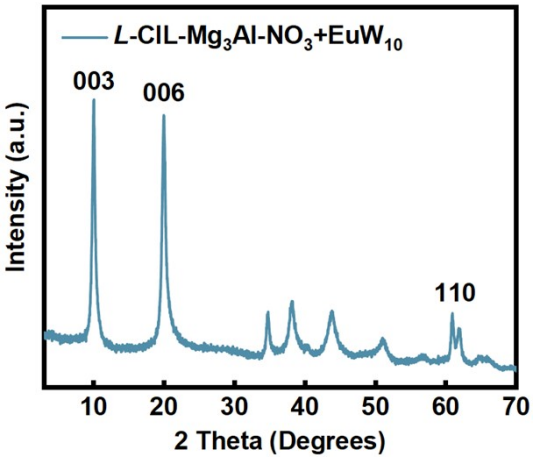

Fig. S20. XRD pattern of the *L*-CIL-Mg_3Al-NO_3 + EuW_{10}.

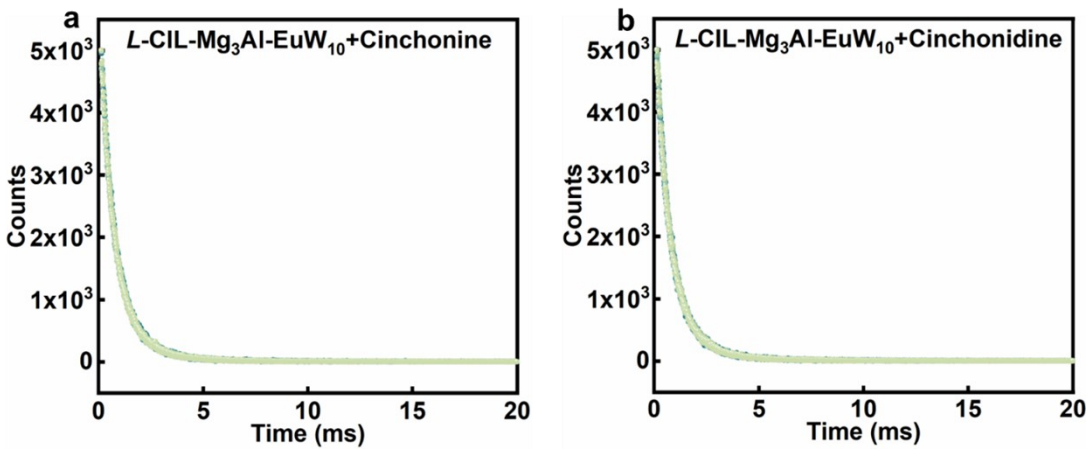

Fig. S21. Luminescence lifetime patterns. *L*-CIL-Mg_3Al-EuW_{10} dispersed in DMF in the presence of (a) Cinchonine and (b) Cinchonidine at 618 nm.

Table S4. Lifetime fitting results. *L*-CIL-Mg_3Al-EuW_{10} in different percent of Cinchonine and Cinchonidine.

Additions (μL)	Lifetime (618 nm/ms)	
	Cinchonine	Cinchonidine
0	1.024	1.011
50	1.012	1.006
100	1.000	0.995
150	1.005	1.004
200	0.997	1.001

[a] 50 mmol additions diluted in 10 mL DMF. [b] Excited at 278 nm.

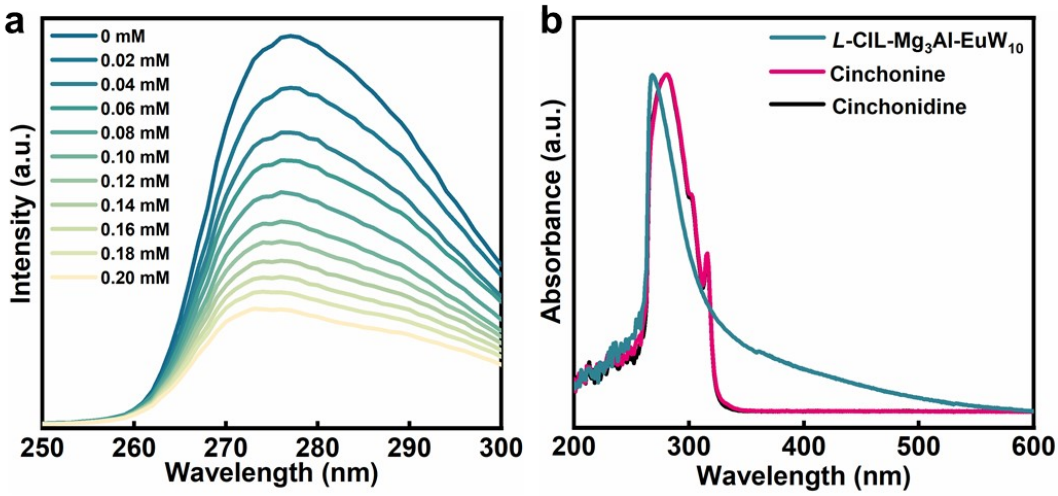

Fig. S22. (a) Excitation spectra of *L*-CIL-Mg_3Al-EuW_{10} suspensions with different concentrations of Cinchonine (λ_{em} = 618 nm). (b) Liquid UV-vis spectra of *L*-CIL-Mg_3Al-EuW_{10}, Cinchonine, and Cinchonidine in DMF.

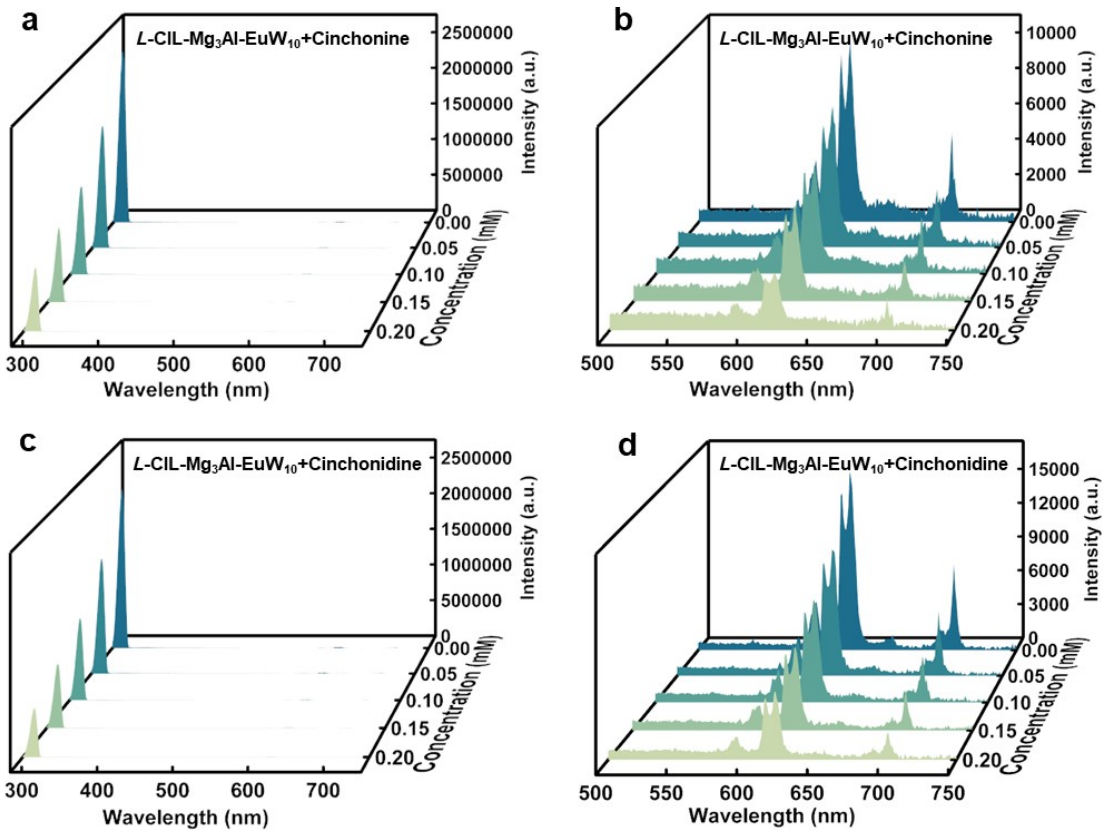

Fig. S23. Quantum yield spectra. Spectra collected during quantum yield analysis for *L*-CIL-Mg_3Al-EuW_{10} dispersed in DMF in the presence of (a, b) Cinchonine and (c, d) Cinchonidine.

Table S5. Quantum yield results. *L*-CIL-Mg_3Al-EuW_{10} in different percent of Cinchonine and Cinchonidine.

Additions [a] (μL)	Quantum yield [b] / %	
	Cinchonine	Cinchonidine
0	1.84	1.93
50	0.76	0.85
100	0.48	0.53
150	0.34	0.36
200	0.20	0.26

[a] 50 mmol additions diluted in 10 mL DMF. [b] Excited at 295 nm.

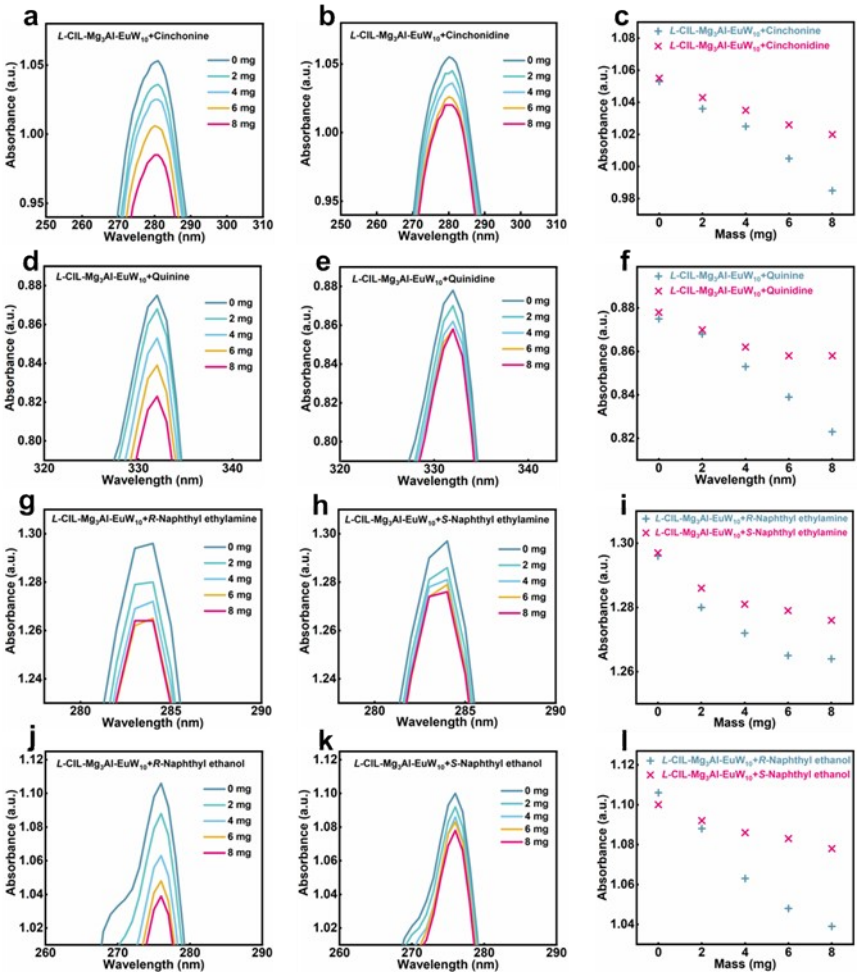

Fig. S24. UV-vis absorption spectra of 3 mL DMF solutions of (a-c) Cinchonine/Cinchonidine, (d-f) Quinine/Quinidine, (g-i) *R*/*S*-Naphthyl ethylamine, (j-l) *R*/*S*-Naphthyl ethanol towards additions of different mass of powder *L*-CIL-Mg_3Al-EuW_{10}. The concentrations of different enantiomer are 0.0001 mmol mL^{-1}.

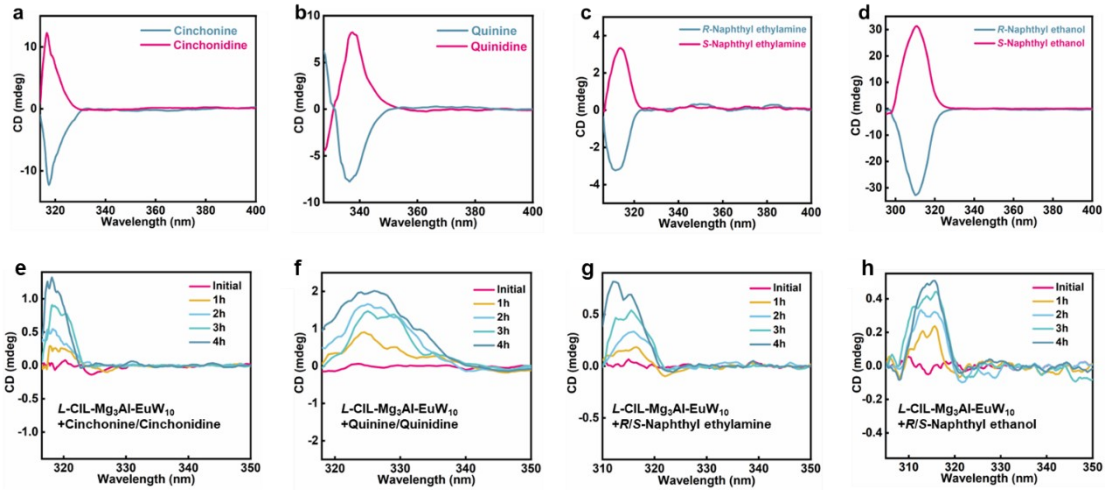

Fig. S25. CD spectra of (a) Cinchonine/Cinchonidine, (b) Quinine/Quinidine, (c) *R*/*S*-Naphthyl ethylamine, (d) *R*/*S*-Naphthyl ethanol and the intensity changes of the equal proportion of the mixture with the additions of *L*-CIL-Mg_3Al-EuW_{10}.

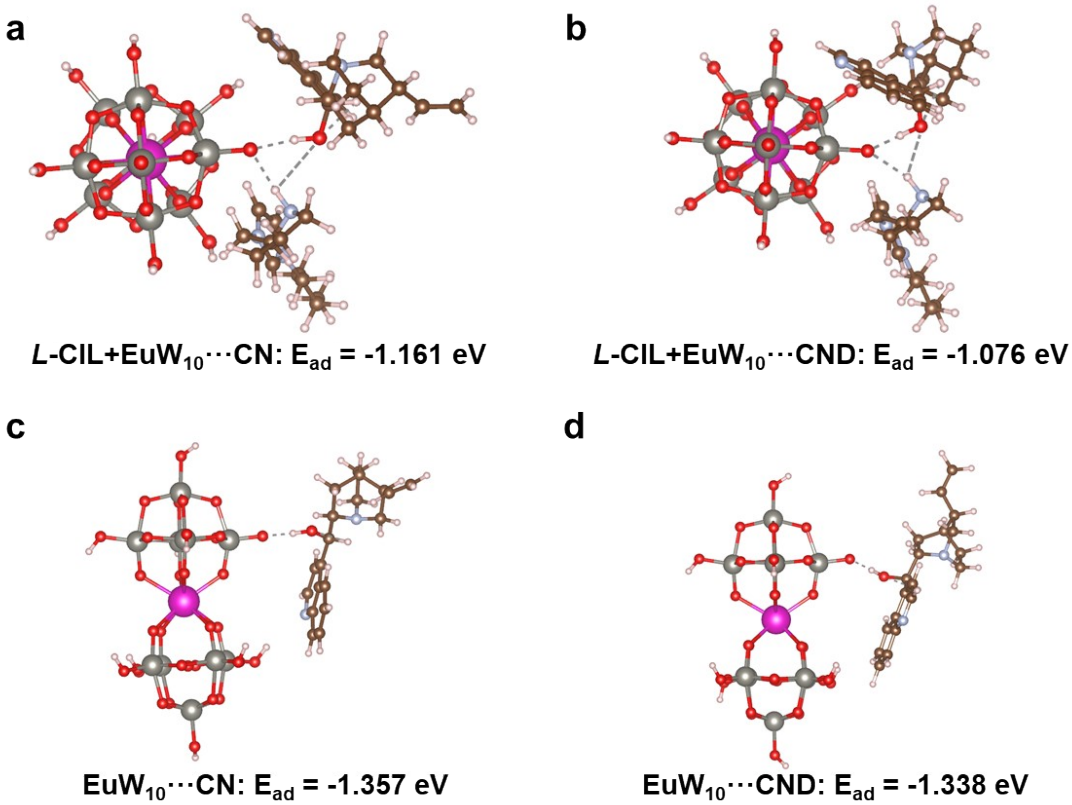

Fig. S26. DFT calculation of the ΔE_{ad} ($\Delta E_{ad} = E_{ad(CN)} - E_{ad(CND)}$) for *L*-CIL+$EuW_{10}$, EuW_{10} adsorbing CN and CND, respectively.

Table S6. Enantioselective recognition in literature. Summary of enantioselective luminescence recognition by coordination compounds.

coordination compounds	categories	analytes	K_{SV}	K_{SV1}/K_{SV2}	centers	references
$[Cl(CO)_3Re(L_1)]_4$	supramolecule	2-amino-1-propanol	7.35(S) 6.02(R)	1.22	ligand	1
$\{[Cd_2(L_2)(H_2O)_2]\cdot 6.5DMF\cdot 3EtOH\}_n$	MOF	2-amino-1-propanol	19.4×10^3(S) 15.5×10^3(R)	1.25	ligand	2
		2-amino-2-phenylethanol	31×10^3(S) 27×10^3(R)	1.17		
		2-amino-3-phenylpropanol	0.68×10^3(S) 0.49×10^3(R)	1.39		
		2-amino-3-methyl-1-butanol	1.66×10^3(S) 0.53×10^3(R)	3.12		
$[(Me_2NH_2)Zn_2(L_5)_{1.5}(H_2O)_2]_n$	MOF	histidine	115(D) 64(L)	1.80	ligand	3
Zn-MOF-C-Tb	MOF	Cinchonine	4.66×10^3 (Cinchonine) 3.45×10^3 (Cinchonidine)	1.35	Tb	4
			4.66×10^3 (Cinchonine) 3.45×10^3 (Cinchonidine)	1.23	ligand	
		N-benzylcinchoninium chloride	4.48×10^3(N-benzylcinchoninium chloride) 3.37×10^3(N-benzylcinchonidinium chloride)	1.33	Tb	
			1.60×10^3(N-benzylcinchoninium chloride) 1.09×10^3(N-benzylcinchonidinium	1.46	ligand	

			chloride)			
		2-amino-1-butanol	5.56×10^3(R) 2.57×10^3(S)	2.16	Tb	
			0.62×10^3(S) 0.18×10^3(R)	3.45	ligand	
		2-amino-1-propanol	72(S) 47(R)	1.53	Tb	
			15.33×10^3(S) 13.01×10^3(R)	1.18	ligand	
L-CIL-Mg_3Al-EuW_{10}	LDHs	Cinchonine	8.37×10^3(Cinchonine) 5.58×10^3(Cinchonidine)	1.60	EuW_{10}	This work
		Quinine	5.53×10^3(Quinine) 4.40×10^3(Quinidine)	1.54		
		Naphthyl ethylamine	9.22×10^3(R) 6.30×10^3(S)	1.46		
		Naphthyl ethanol	5.98×10^3(R) 3.31×10^3(S)	1.81		